Available online at www.sciencedirect.com
SCIENCE DIRECT®
Chemical Physics Letters 385 (2004) 498–501
CHEMICAL PHYSICS LETTERS
www.elsevier.com/locate/cplett

An investigation of the $6a_g$ inner valence orbital electron density of the antimicrobial agent diacetyl by binary (e,2e) spectroscopy ☆

G.L. Su [a,b,*], X.G. Ren [a,b], S.F. Zhang [a,b], C.G. Ning [a,b], H. Zhou [a,b], B. Li [a,b], G.Q. Li [a,b], J.K. Deng [a,b], Y. Wang [a,b], Y. Zheng [c]

[a] Department of Physics, Tsinghua University, Beijing 100084, PR China
[b] Key Laboratory for Quantum Information and Measurements, MOE, PR China
[c] Department of Chemistry, The University of British Columbia, Vancouver, BC V6T 1Z1, Canada

Received 14 November 2003; in final form 10 January 2004

Abstract

We report here the first measurements of the complete valence shell binding energy spectra and the $6a_g$ inner valence orbital momentum profile of the antimicrobial agent diacetyl, also known as 2,3-butanedione ($CH_3COCOCH_3$), using a high-resolution binary (e,2e) electron momentum spectroscopy, at an impact energy of 1200 eV plus the binding energy, and using symmetric non-coplanar kinematics. The experimental momentum profile of the $6a_g$ inner valence orbital is compared with Hartree–Fock (HF) and density functional theory (DFT) calculations. The experimental measurement is quite well described by the HF and DFT calculations.

1. Introduction

Electron momentum spectroscopy (EMS), with symmetric non-coplanar geometry based on a binary (e,2e) ionization reaction, has developed rapidly since the pioneer research by Amaldi et al. [1] and Weigold et al. [2]. While the unique ability of EMS to essentially measure electron momentum distributions of individual orbitals has made it into a powerful experimental tool for investigating the electronic structures of atoms, molecules and condensed matter [3–10], applications of EMS to larger molecules have proved to be more challenging. Now the EMS has become practical to apply EMS to studies of larger molecules of biological and pharmaceutical interest [7,11–13]. In particular, EMS measurements of the momentum profiles for individual orbitals in atoms and molecules have taken significant improvements in theoretical quantum chemistry in computing electron correlation effects (i.e., developments of generalized gradient approximations in density function theory (DFT)), to permit measurements on larger molecules together with meaningful interpretation of the results. The extension of EMS to biomolecules and pharmaceuticals is particularly appealing because of possible applications for experimental testing, validation and evaluation of computational chemical methods used for applications such as computer-aided drug design and the prediction of reactivity. Several EMS studies of larger biologically important molecules such as the aminoacid glycine [7,11] and urotropine [14] have been reported together with quantum chemical calculations using Hartree–Fock (HF) and DFT methods.

Diacetyl, also known as 2,3-butanedione ($CH_3COCOCH_3$), has received much interest because of the antimicrobial activity against *Escherichia coli*, *Listeria monocytogenes* and *Staphylococcus aureus* [15]. It has been widely studied by photoelectron spectroscopy (PES) [16,17] and also analyzed by two new spectro-

☆ Project supported by the National Natural Science Foundation of China under Grant Nos. 19854002, 19774037 and 10274040 and the Research Fund for the Doctoral Program of Higher Education under Grant No. 1999000327.
* Corresponding author. Fax: +86-10-62781604.
E-mail addresses: sg101@mails.tsinghua.edu.cn (G.L. Su), djk-dmp@mail.tsinghua.edu.cn (J.K. Deng).

0009-2614/$ - see front matter © 2004 Elsevier B.V. All rights reserved.
doi:10.1016/j.cplett.2004.01.019

photometric and fluorimetric methods in yogurt [18]. Recently, diacetyl was studied over the 0–18 eV energy range by EMS whose energy resolution and momentum resolution were about 1.40 eV (FWHM) and 0.23 a.u. at an impact energy of 1200 eV [19]. In this Letter, we report the complete binding energy spectra (1–40 eV) of $CH_3COCOCH_3$ and electron momentum profile of its $6a_g$ inner valence molecular orbital with the 1.15 eV (FWHM) energy resolution and about 0.1 a.u. momentum resolution. The inner valence region provides a very sensitive test of the many-body calculations that take initial and final states correlations into account [20]. The measured momentum profile is compared with the HF and DFT calculations.

2. Theoretical background

Electron momentum spectroscopy is based on a so-called binary (e,2e) experiment in the symmetric non-coplanar geometry. Under collision conditions of high impact energy and high momentum transfer, the ionized electron essentially undergoes a clean 'knock-out' collision. In this situation several approximations, of which the most important are the binary encounter approximation and the plane wave impulse approximation (PWIA), provide a very good description of the collision [3]. Under the approximations, using symmetric non-coplanar geometry, the kinematic factors are effectively constant [3] and the EMS cross-section for randomly oriented molecules is then given [3] by:

$$\sigma_{\mathrm{EMS}} \propto \int \mathrm{d}\hat{p} \left| \left\langle \boldsymbol{p} \Psi_{\mathrm{f}}^{N-1} \middle| \Psi_{\mathrm{i}}^{N} \right\rangle \right|^2, \tag{1}$$

where $\boldsymbol{p}$ is the momentum of the target electron state prior to electron ejection and $|\Psi_{\mathrm{f}}^{N-1}\rangle$ and $|\Psi_{\mathrm{i}}^{N}\rangle$ are the total electronic wavefunctions for the final ion state and the target molecule ground (initial) state, respectively. The overlap of the ion and neutral wavefunctions in Eq. (1) is known as the Dyson orbital, while the square of this quantity is referred to as an ion-neutral overlap distribution (OVD). Thus, the (e,2e) cross-section is essentially proportional to the spherical average of the square of the Dyson orbital in momentum space.

Eq. (1) is greatly simplified by using the target Hartree–Fock approximation (THFA). Within the THFA, only final (ion) state correlation is allowed and the many-body wavefunctions $|\Psi_{\mathrm{f}}^{N-1}\rangle$ and $|\Psi_{\mathrm{f}}^{N}\rangle$ are approximated as independent particle determinants of ground state target HF orbitals in which case Eq. (1) reduces to

$$\sigma_{\mathrm{EMS}} \propto \int \mathrm{d}\Omega \left| \psi_j(\boldsymbol{p}) \right|^2, \tag{2}$$

where $\psi_j(\boldsymbol{p})$ is the one-electron momentum space canonical HF orbital wavefunction for the jth electron, corresponding to the orbital from which the electron was ionized. The $\int \mathrm{d}\Omega$ represents the spherical average due to the randomly oriented target. The integral in Eq. (2) is known as the spherically averaged one-electron momentum distribution. To this extent EMS has the ability to image the electron density in individual 'orbitals' selected according to their binding energies.

Eq. (1) has recently been re-interpreted [21] in the context of Kohn–Sham density functional theory (DFT) and the Target Kohn–Sham Approximation (TKSA) gives a result similar to Eq. (2) but with the canonical HF orbital replaced by a momentum space Kohn–Sham orbital $\psi_j^{\mathrm{KS}}(\boldsymbol{p})$:

$$\sigma_{\mathrm{EMS}} \propto \int \mathrm{d}\Omega \left| \psi_j^{\mathrm{KS}}(\boldsymbol{p}) \right|^2. \tag{3}$$

It should be noted that accounting of electron correlation effects in the target ground state is included in the TKSA via the exchange correlation potential. A more detailed description of the TKSA–DFT method may be found elsewhere [21].

THFA calculations of the momentum profiles were carried out using Eq. (2). DFT calculations were carried out using the GAUSSIAN 98 program with the B3LYP functionals [22–24]. The geometry of diacetyl reported by Hagen and Hedberg [25] has been used for all the calculations. In order to compare the calculated cross-sections with the experimental electron momentum profiles, the effects of the finite spectrometer acceptance angles in both θ and ϕ ($\Delta\theta = \pm 0.6°$ and $\Delta\phi = \pm 1.2°$) were included using the Gaussian-weighted planar grid method [26].

3. Experimental method

A detailed description of the present EMS constructed at Tsinghua University has been reported [27]. Therefore, it is described briefly here. Two hemispherical electron energy analyzers are mounted on two independent horizontal concentric turntables inside a mu-metal shielded vacuum system. In the present work, the polar angles of both analyzers are kept fixed at 45°. One analyzer turntable is kept in a fixed position, while the other one is rotated over a range of ±30°. The energy range of each analyzer was set at 600 ± 4 eV with a pass energy of 50 eV. The energy resolution, as well as the binding energy scale, was measured directly by using argon 3p as a calibration gas. The coincidence energy resolution of the spectrometer was measured to be 1.15 eV FWHM. The experimental momentum resolution is estimated to be ~0.1 a.u. from a consideration of the argon 3p angular correlation. The sample of diacetyl (99.0% purity) was used without further purification. No impurities were evident in the binding energy spectra.

4. Results and discussion

Diacetyl contains 46 electrons and has C_{2h} symmetry point group. According to molecular orbital theory, the ground state electronic configuration can be written as

Inner valence

$$(\text{core})^{12}(4a_g)^2(4b_u)^2(5a_g)^2(5b_u)^2(6a_g)^2$$

Outer valence

$$(6b_u)^2(7a_g)^2(1a_u)^2(7b_u)^2(1b_g)^2(8a_g)^2(8b_u)^2(9a_g)^2(2a_u)^2 \times (2b_g)^2(9b_u)^2(10a_g)^2$$

The valence-shell contains 17 molecular orbitals and can be divided into two sets of five inner valence and 12 outer valence orbitals. The order of these valence orbitals has been established, both by PES and molecular calculations [17].

In order to obtain the experimental momentum profiles, 12 binding energy spectra over the energy range of 1–40 eV were collected at the out-of-plane azimuth angles $\varphi = 0°, 1°, 2°, 3°, 4°, 5°, 7°, 10°, 12°, 14°, 17°$ and 22° in a series of sequential repetitive scans. Fig. 1 shows the binding energy spectra of diacetyl in the range 1–40 eV for measurements at $\varphi = 0°$ and $\varphi = 10°$ (incident energy of 1200 eV plus the binding energy). The spectra in Fig. 1 were fitted with a set of individual Gaussian peaks. The fitted Gaussians for individual peaks are indicated by dashed lines while their sum, i.e., the overall fitted spectra, are represented by the solid lines. Except for the last peak at 32.7 eV, the widths of the peaks are combinations of the EMS instrumental energy resolution and the corresponding Franck–Condon widths derived from high resolution PES data [17] and the relative energy values of the peaks are given by the relative ionization energies determined by high resolution PES. The ionization potential value and the width of the last peak are determined by our EMS experiment. The differences of the orbitals in FWHM are due to the vibrational broadening of the lines.

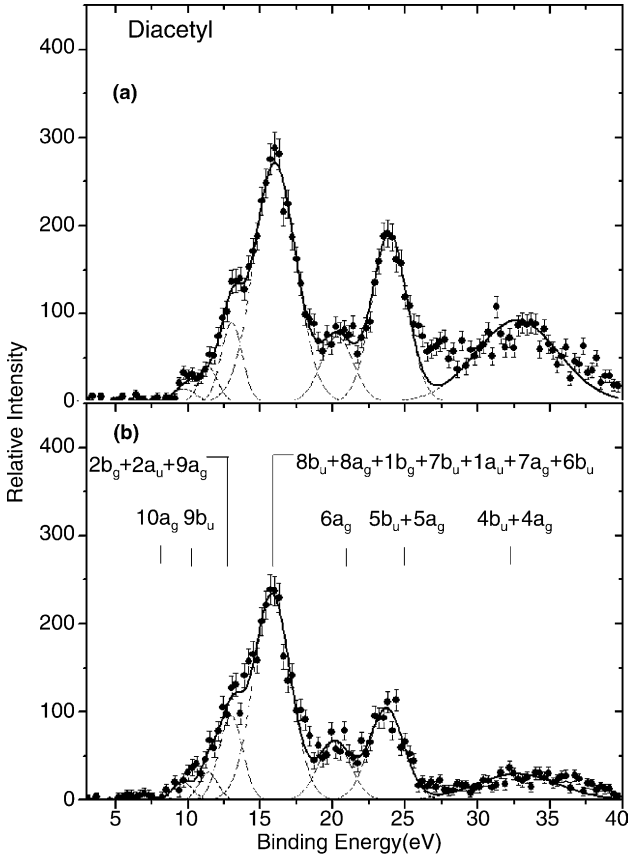

Fig. 1. Valence shell binding energy spectra for diacetyl at: (a) $\varphi = 0°$; (b) $\varphi = 10°$. The dashed and solid lines represent individual and summed Gaussian fits, respectively.

The PES spectrum of the 12 outer valence and three inner valence region has been reported by Niessen and co-workers [17]. In this work, the vertical ionization potentials of the $10a_g$ and $9b_u$ orbitals were determined to be 9.6 and 11.5 eV, respectively. However, the three orbitals, $2b_g$, $2a_u$ and $9a_g$, whose vertical ionization potentials were from 12.6 to 14.0 eV, were not well resolved. The same is true of the next three orbitals, $8b_u$, $8a_g$ and $1b_g$, with the vertical ionization potentials from 14.5 to 15.2 eV. In sequence, 16.0, 16.0, 16.5, 17.4, 20.6, 24.0 and 24.0 eV were assigned to the vertical ionization potentials of the $7b_u$, $1a_u$, $7a_g$, $6b_u$, $6a_g$, $5b_u$ and $5a_g$ orbitals.

In the EMS binding energy spectra of Fig. 1, however, only seven structures could be well identified. The vertical ionization potentials of the two outer valence orbitals, $10a_g$ and $9b_u$ are at 9.6 and 11.4 eV. The average vertical ionization potentials of the $(2b_g + 2a_u + 9a_g)$ and $(8b_u + 8a_g + 1b_g + 7b_u + 1a_u + 7a_g + 6b_u)$ outer valence orbital sums are determined to be 12.8 and 15.8 eV, respectively. The band located at 20.4 eV corresponds to the removal of an electron from the $6a_g$ inner valence orbital. In sequence, 23.8 and 32.7 eV are assigned to the average vertical ionization potentials of $(5b_u + 5a_g)$ and $(4b_u + 4a_g)$ inner valence orbital sums. Thus, the EMS experimental binding energy spectra are consistent of the PES values [17]. It should also be noted that no results before have been reported for the ionization potential values of the $4b_u$ and $4a_g$ orbitals as far as we know, although our EMS experiment could not resolve the two orbitals due to the insufficient resolution of the EMS.

Experimental momentum profiles (XMPs) have been extracted by deconvolution of the sequentially obtained angular-correlated binding energy spectra, and therefore the relative normalization for the different transitions is maintained. For the $6a_g$ inner valence orbital, the various theoretical momentum profiles (TMPs) are obtained with the methods described above and the experimental instrumental angular resolutions have been incorporated in the calculations using the UBC RESFOLD

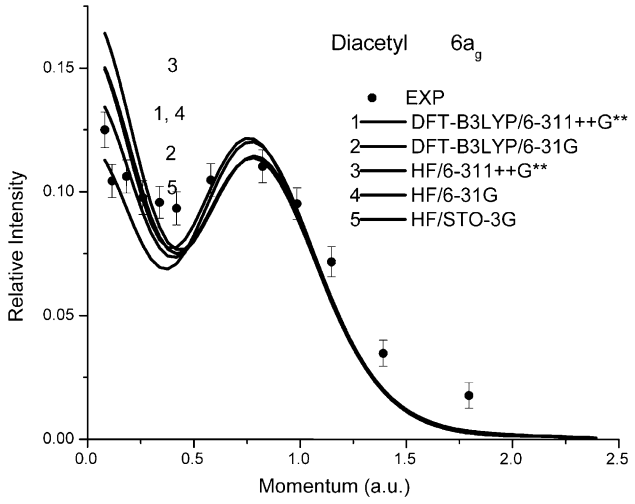

Fig. 2. The experimental and calculated momentum distributions for the $6a_g$ inner valence orbital of diacetyl. The TMPs are calculated by using HF (curves 3–5) with the 6-311G++**, 6-31G and STO-3G basis sets and DFT-B3LYP (curves 1 and 2) methods with the 6-311++G** and 6-31G basis sets.

program based on the GW–PG methods [26]. The experimental momentum distribution is compared, in Fig. 2, with the five theoretical momentum profiles calculated using HF method (curves 3–5) with the 6-311++G**, 6-31G and STO-3G basis sets, and DFT-B3LYP (curves 1 and 2) method with the 6-311++G** and 6-31G basis sets. It can be seen that all the five calculations using the DFT and HF methods well reproduce the XMP in high momentum region above 0.5 a.u. But the calculation results (curves 3, 1 and 4), in particular the HF method with the 6-311++G** basis, slightly overestimate the observed intensity in the low momentum range near the zero momentum. The full details of the experimental results and the associated theoretical analysis for diacetyl will be reported later.

5. Summary

In summary, we report the first measurements of the complete valence shell binding spectra and the $6a_g$ inner valence momentum profile of the antimicrobial agent diacetyl. The experimental momentum profile of the inner valence orbital is also compared with the theoretical momentum distributions calculated using HF and DFT methods with various basis sets. The experimental measurement is quite well described by the HF and DFT calculations.

References

[1] U. Amaldi, A. Egidi, R. Marconero, G. Pizzella, Rev. Sci. Instrum. 40 (1969) 1001.
[2] E. Weigold, S.T. Hood, O.J.O. Teubner, Phys. Rev. Lett. 20 (1973) 475.
[3] I.E. McCarthy, E. Weigold, Rep. Prog. Phys. 91 (1991) 789, and references therein.
[4] C.E. Brion, in: T. Andersen (Ed.), Proceedings of Physics of Electronic and Atomic Collisions (XVIII ICPEAC), AIP Press, New York, 1993, p. 350, and references therein.
[5] K.T. Leung, Sci. Prog., Oxford 75 (1991) 157.
[6] M.A. Coplan, J.H. Moore, J.P. Doering, Rev. Mod. Phys. 66 (1994) 985.
[7] Y. Zheng, J.J. Neville, C.E. Brion, Science 270 (1995) 786.
[8] M. Vos, I.E. McCarthy, Rev. Mod. Phys. 67 (1995) 713.
[9] J.K. Deng, G.Q. Li, J.D. Huang, et al., Chem. Phys. Lett. 313 (1999) 134.
[10] J.K. Deng, G.Q. Li, Y. He, et al., J. Chem. Phys. 21 (2000) 882.
[11] J.J. Neville, Y. Zheng, C.E. Brion, J. Am. Chem. Soc. 118 (1996) 10533.
[12] I.V. Litvinyuk, Y. Zheng, C.E. Brion, Chem. Phys. 253 (2000) 41.
[13] J.J. Neville, Y. Zheng, B.P. Hollebone, N.M. Cann, C.E. Brion, C.-K. Kim, S. Wolf, Can. J. Phys. 74 (1996) 773.
[14] I.V. Litvinyuk, J.B. Young, Y. Zheng, G. Copper, C.E. Brion, Chem. Phys. 263 (2001) 195.
[15] R. Lanciotti, F. Patrignani, F. Bagnolini, M.E. Guerzoni, F. Gardini, Food Microbiol. 20 (2003) 537.
[16] K. Kimura, S. Katsumata, Y. Achiba, T. Yamazaki, S. Iwata, Handbook of HeI Photoelectron Spectra of Fundamental Organic Molecules, Japan Scientific Society, Tokyo, 1981.
[17] W. Von. Niessen, G. Bieri, L.L. Åsbrink, J. Electron. Spectrosc. Relat. Phenom. 21 (1980) 175.
[18] E.J.G. Hernández, R.G. Estepa, I.R. Rivas, Food Chem. 53 (1995) 315.
[19] M. Takahashi, T. Saito, J. Hiraka, Y. Udagawa, J. Phys. B: At. Mol. Opt. Phys. 36 (2003) 2539.
[20] J.K. Deng, G.Q. Li, Y. He, et al., Chin. Phys. Lett. 17 (2000) 795.
[21] P. Duffy, D.P. Chong, M.E. Casida, D.R. Salahub, Phys. Rev. A 50 (1994) 4704.
[22] C. Lee, W. Yang, R.G. Parr, Phys. Rev. B 37 (1988) 785.
[23] B. Miehlich, A. Savin, H. Stoll, H. Preuss, Chem. Phys. Lett. 157 (1989) 200.
[24] A.D. Becke, J. Chem. Phys. 98 (1996) 5648.
[25] K. Hagen, K. Hedberg, J. Am. Chem. Soc. 95 (1973) 8266.
[26] P. Duffy, M.E. Casida, C.E. Brion, D.P. Chong, Chem. Phys. 159 (1992) 347.
[27] Y. Zheng, W.N. Pang, R.C. Shang, X.J. Chen, C.E. Brion, T.K. Ghanty, E.R. Davidson, J. Chem. Phys. 111 (1999) 9526.